Azabuckybowl-Based Molecular Tweezers as C_{60} and C_{70} Receptors

Motoki Takeda,[†] Satoru Hiroto,[†*] Hiroki Yokoi,[†] Sangsu Lee,[‡] Dongho Kim,[‡*] and Hiroshi Shinokubo[†*]

†Department of Molecular and Macromolecular Chemistry, Graduate School of Engineering, Nagoya University, Furo-cho, Chikusa-ku, Nagoya, Aichi 464-8603, Japan.

‡Department of Chemistry, Yonsei University, 50 Yonsei-ro, Seodaemoon-gu, Seoul 03722, Korea

ABSTRACT: We designed and synthesized molecular tweezers consisted of nitrogen-embedded buckybowl subunits. The judicious choice of the covalent linkers modulated their binding strength with C_{60} or C_{70} in solution. Titration studies by optical and ^{1}H NMR analysis revealed a 1:1 composition of the resulting complexes. X-Ray diffraction analysis elucidated their solid-state structures in which two azabuckybowl units surround one molecule of fullerenes. The large association constants stabilize the complexes under redox reactions and purification process on silica-gel column chromatography. The linker enabled to tune the cavity size for binding fullerenes, achieving complementary fullerene host between C_{60} and C_{70}: the carbazole-bridged dimer preferentially associates with C_{70} over C_{60}, while the phenanthrene-bridged dimer interacts with C_{60} more strongly than C_{70}. Electrochemical analysis in combination with DFT calculations indicated the existence of intermolecular charge-transfer interactions between the buckybowl units and fullerenes. Nonlinear optical measurements exhibited that the two-photon absorption cross-section values of the molecular tweezers are enhanced upon association with fullerenes.

Introduction

Molecular tweezers, *i.e.*, noncyclic hosts capable of binding a guest molecule via non-covalent interactions such as π–π interactions, hydrogen bonds, and metal coordination, have been widely investigated as molecular sensors.[1,2] Their structural flexibility enables reversible binding that has been applied to supramolecular polymers and drug delivery systems.[3] Among a number of molecular tweezers, fullerene receptors have been intensively studied in order to selectively extract C_{60} or other fullerenes from carbon soot.[4,5] To date, planar molecules such as porphyrins have been employed for popular hosts in this context.[6-8] However, the planar structure does not adapt the complexation with spherical fullerenes, thus diminishing association constants and hence through-space electronic communication.

Against this background, bowl-shaped π-conjugated molecules such as subphthalocyanines,[9] subporphyrins,[10] and corannulenes[11] have been investigated as platforms to host C_{60}.[12] However, their relatively low electron-donating properties compared with that of porphyrins usually requires the presence of additional electron-donating substituents in order to enhance their binding ability toward fullerenes in solution. Alternatively, the "buckycatcher" strategy with the aid of two corannulene units is successful to enhance the association with C_{60}, as reported by Sygula and co-workers (Figure 1).[13-15]
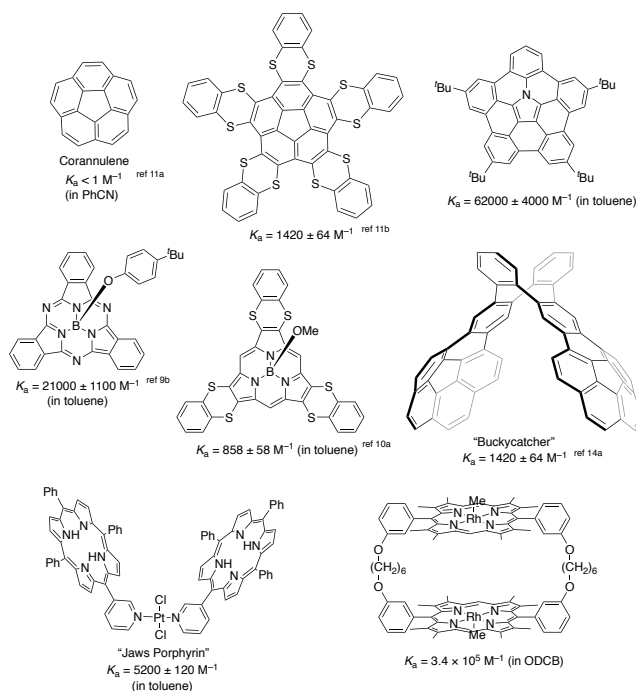

Figure 1. Fullerene receptors based on bowl-shaped π-conjugated molecules together with their association constants toward C_{60}.

Recently, we and Nozaki group have independently synthesized the pyrrolic nitrogen embedded azabuckybowl **1** (Figure 1).[16] We also disclosed that its concave surface and remarkable electron-donating properties lead to a large association constant with C_{60} in solution (3800 M^{-1} in *o*-dichlorobenzene and 62000 ± 4000 M^{-1} in toluene). The resulting inclusion complex exhibited intermolecular charge-transfer interactions between the azabuckybowl and C_{60}. With this electron-donating bowl-shaped C_{60} receptor in hand, we

designed molecular tweezers to construct supramolecular donor–acceptor–donor (D–A–D) systems upon binding with C_{60} and C_{70}. Such D–A–D systems should generate quadrupolar characteristics due to intermolecular charge transfer, which should enhance the two-photon absorption (TPA) cross-section values.[17,18] TPA properties using host-guest D–A–D systems have not been examined experimentally.[19] Here we report the synthesis of two novel molecular tweezers, which showed complementary binding of C_{60} and C_{70}. In addition, we demonstrated that TPA properties of the host molecules were modulated by binding with fullerenes.

Results and Discussions

Synthesis and characterizations of azabuckybowl dimers. We chose fused biphenylene linkers as a π-spacer in order to connect two azabuckybowl units (Scheme 1). The size of the cavity, i.e., the space between the two π-bowls, can be readily tuned by a judicious choice of the moiety X. In order to choose suitable π-spacers, we performed density functional theory (DFT) calculations at the M06-2X/6-31G(d) level of theory. The calculations predicted that the use of 3,6-carbazole and 3,6-phenanthrene spacers generated tweezers (**2a** and **2b**) with a suitable cavity for C_{60}. The synthesis of **2a** (50%) and **2b** (68%) was accomplished via the cross-coupling of 2-borylated azabuckybowl **3**, which was prepared according to our previous report,[16a] and 3,6-dibromocarbazole or 3,6-diiodophenanthrene.
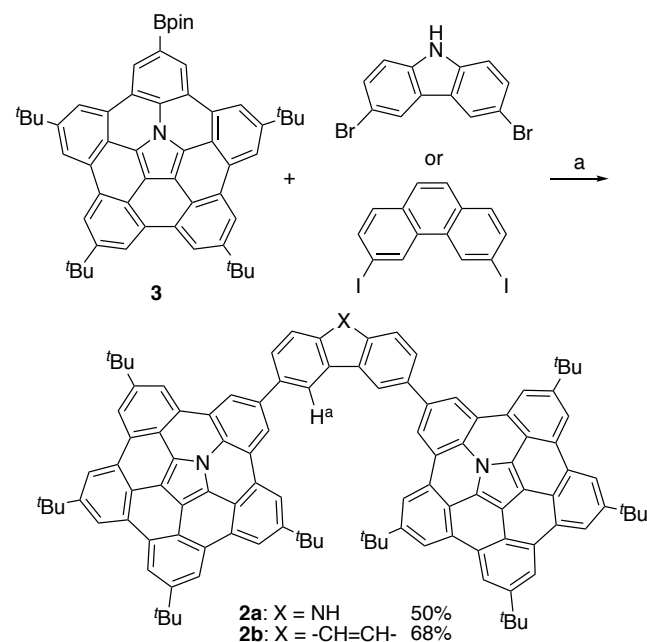
Scheme 1. Synthesis of azabuckybowl dimers.

Figure 2a shows the UV/Vis absorption and emission spectra of **1**, **2a**, and **2b** in CH_2Cl_2, which revealed slight bathochromic shifts for the lowest energy absorption bands and emission maxima of **2a** and **2b** compared to that of **1**. The fluorescent quantum yields (Φ_f) of **2a** (0.18) and **2b** (0.18) are almost identical to that of **1** (0.17).
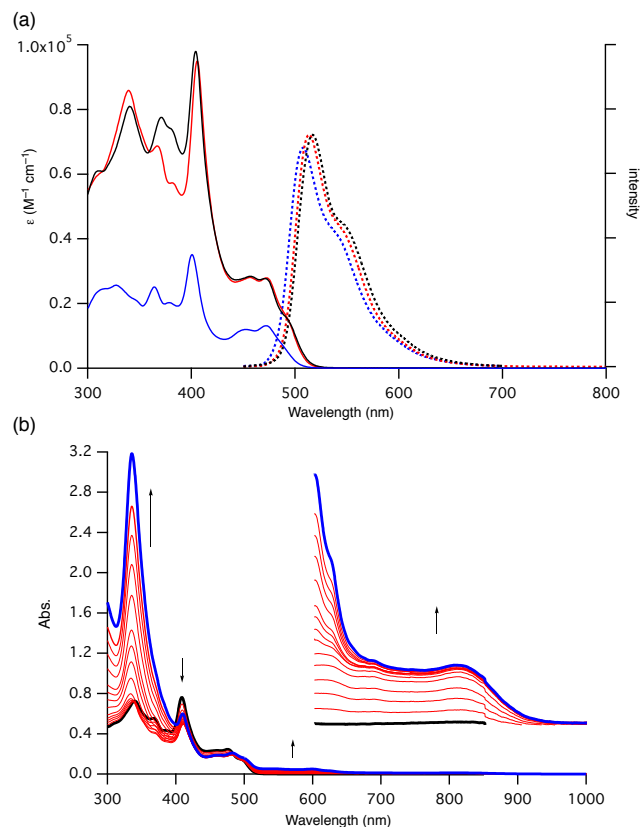

Figure 2. (a) UV/Vis absorption (solid line) and emission (dotted line) spectra of **1** (blue), **2a** (red), and **2b** (black) in CH_2Cl_2. (b) Change of the UV/Vis/NIR absorption spectra of **2a** upon gradual addition of C_{60} in toluene.

Binding behaviors with fullerenes. To examine the potential utility of **2a** and **2b** as fullerene receptors, titration experiments were carried out. A gradual change of the absorption bands of **2a** in toluene was observed upon addition of C_{60} (Figure 2b). In particular, the generation of a broad absorption band in the near-IR region under concomitant quenching of the emission (Figure S7) was observed, indicative of the existence of intermolecular electronic interactions between **2a** and C_{60}. Judging from a Job's plot, a 1:1 stoichiometry between **2a** and C_{60} predominates in solution.

The binding behavior of **2a** with C_{60} was monitored by its ^1H NMR spectrum. Upon addition of 0.5 equiv of C_{60} to a toluene-d_6 solution of **2a**, broadening of the aromatic proton signals was observed. In contrast, upon addition of 1.0 equiv of C_{60}, sharp, upfield shifted signals were observed (Figure 3a). In particular, a singlet peak for the carbazole linker (H^a in Scheme 1) was observed at 7.99 ppm, which is upfield shifted relative to that of **2a** (8.48 ppm) due to the shielding effect of C_{60}. Moreover, the symmetric feature of the carbazole proton signals confirms a 1:1 composition in solution.
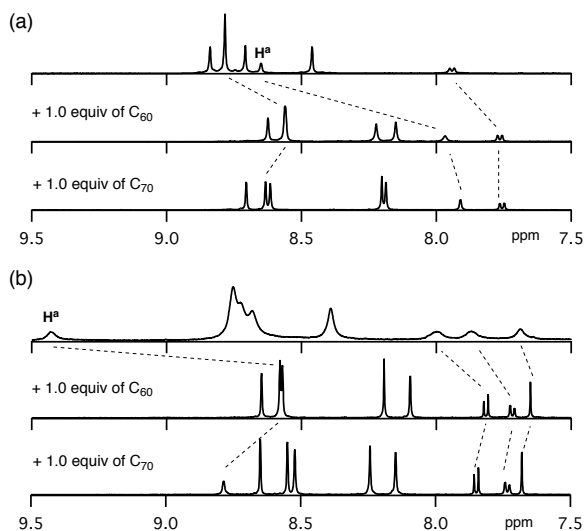
Figure 3. ^{1}H NMR spectra of (a) **2a** and (b) **2b** in toluene-d_8, containing 0 equiv of fullerenes (top), 1.0 equiv of C_{60} (middle), and 1.0 equiv of C_{70} (bottom).

Table 1. Summarized association constants of 1, 2a, and 2b.

compound	association constants (M^{-1})		
	C_{60}		C_{70}
	toluene	ODCB	toluene
1	$(6.2 \pm 0.4) \times 10^4$	3.8×10^3	–
2a	$(4.4 \pm 0.4) \times 10^7$	$(3.0 \pm 0.3) \times 10^5$	$(7.0 \pm 3.1) \times 10^8$
2b	$(3.0 \pm 1.1) \times 10^8$	$(2.2 \pm 0.7) \times 10^6$	$(6.3 \pm 0.8) \times 10^7$

Similar spectral changes were also observed in the case of **2b** (Figure S9, S10). On the basis of titration experiments, association constants of $(3.0 \pm 0.3) \times 10^5$ (**2a**) and $(2.2 \pm 0.7) \times 10^6$ M^{-1} (**2b**) were determined in *o*-dichlorobenzene (ODCB). The larger association constant for **2b** than that of **2a** indicates that **2b** has a more suitable cavity to catch C_{60}. The binding strength depends on the solvent (Table 1). In toluene, the association constant of **2b** $[(3.0 \pm 1.1) \times 10^8 \, M^{-1}]$ is by a factor of 50,000 higher than that of Jaw's porphyrins, and comparable with rhodium(III) porphyrin cages $(3.4 \times 10^5 \, M^{-1}$ in ODCB and $2.4 \times 10^7 \, M^{-1}$ in benzene).[20,21] The stability of **2b•C_{60}** was substantially high in CH_2Cl_2, enabling purification of the complex by column chromatography on silica gel.

These azabuckybowl tweezers also showed efficient binding with C_{70} in the solution state.[22] The similar tendencies for UV/vis absorption and emission spectroscopy were observed upon titration experiments with **2a** and **2b** (Figure S8, S11). 1:1 Stoichiometries of the binding complexes were confirmed by Job's plot analysis. According to these titration studies, the binding constants were determined to be $(7.0 \pm 3.1) \times 10^8 \, M^{-1}$ for **2a** and $(6.3 \pm 0.8) \times 10^7$ M^{-1} for **2b** in toluene. Consequently, the binding preference of the hosts was reversed in the case of C_{70} compared to the case of C_{60}. Figure 3b displays ^{1}H NMR spectra of **2a** and **2b** in the presence of C_{70}. As well as the case of C_{60}, the addition of C_{70} induced upfield shifts of all aromatic protons of **2a** or **2b**. In particular, the signal of H[a] shows larger shifts than others, indicating the similar binding mode for C_{70} to that of C_{60}. Notably, H[a] of **2a•C_{70}** appeared in the lower field than that of **2a•C_{60}**. This situation is opposite to those

observed in the case of **2b**. The larger shift of H[a] indicates that a fullerene unit places closer to a linker. This tendency also confirms the more efficient binding of C_{70} for **2a** than **2b**.

Table 2. Summarized diffusion coefficients and Stokes–Einstein radii of 2a, 2b, 2b•C_{60}, and 2b•C_{60}.

	2a	**2a•C_{60}**	**2a•C_{70}**	**2b**	**2b•C_{60}**	**2b•C_{70}**
D^a	5.12	5.34	6.17	4.74	5.71	5.15
r^b	7.36	7.06	6.10	7.95	6.56 (7.87)[c]	7.33 (7.84)[c]

a: unit: $10^{-10} \, m^2 \, K^{-1}$, b: unit: Å, c: calculated from X-ray data

The formation of 1:1 complexes in solution was also confirmed by 2D DOSY NMR and ESI-TOF MS analysis (Figure S14, S15). Table 2 summarizes diffusion coefficients (D) and Stokes–Einstein radii (r) for **2a**, **2a•C_{60}**, **2a•C_{70}**, **2b**, **2b•C_{60}**, and **2b•C_{70}** obtained by DOSY experiments. The diffusion coefficients of **2a** and **2b** were increased upon binding C_{60} and C_{70}. The increased D values indicate that **2a** and **2b** shrank by folding azabuckybowl units upon binding fullerenes. The radii were estimated to be 7.06 for **2a•C_{60}** and 6.60 Å for **2b•C_{60}**, which are consistent with the 1:1 binding complexes. In the case of **2a**, binding C_{70} also increased the D value as in the case of C_{60}. On the other hand, the diffusion coefficient became smaller for **2b** on binding C_{70} than that for C_{60}. Considering the smaller cavity of **2b** for C_{70}, the binding C_{70} increase the volume of the complex, resulting in decrease of diffusion coefficient. In the case of **2a**, the cavity was more adaptable for C_{70} than C_{60}, resulting in the larger D value.

The solid-state structure of **2b•C_{60}** and **2b•C_{70}** were unambiguously determined by single-crystal X-ray diffraction analysis (Figure 4), which revealed 1:1 compositions similar to those observed in solution. In the crystalline state, C_{60} and the azabuckybowl units mutually interact in a concave-convex fashion.[23,24] The penetration depth of C_{60} into **2b** measured from the centroid of the pyrrole ring of **2b** to the centroid of C_{60} is 6.83 Å, which is consistent with that of **1**. The closest distance between C_{60} and an azabuckybowl unit was 3.14 Å. The center of C_{60} is displaced relative to the position of the phenanthrene linker (Figure 4b). Noted that the C_{60} molecule in crystal is disordered, indicating that the rotation of C_{60} is not restricted. On the other hand, C_{70} molecule is fixed and showed no rotation in crystal. Notably, the C_{70} is obliquely placed to the C_2 symmetrical axis of **2b**. The penetration depths defined as the distance between the centroids of the pyrrole ring and the center of C_{70} are 7.345 Å and 7.055 Å, which are longer than that in the case of C_{60}. The closest distances between each azabuckybowl unit and C_{70} are 3.147 Å and 3.173 Å, respectively. Both are within the sum of van der Waals radii of carbon atoms, indicating the presence of π–π interaction. The angle Z1-X1-Z2 was 136.9 Å, narrower than that of **2b•C_{60}** (143.4°)(Table 3). The narrower angle indicates that the host covers the smaller convex surface of the fullerene, providing larger volume of the complex. This result is consistent with the larger diffusion coefficient of **2b•C_{70}** than **2b•C_{60}**.
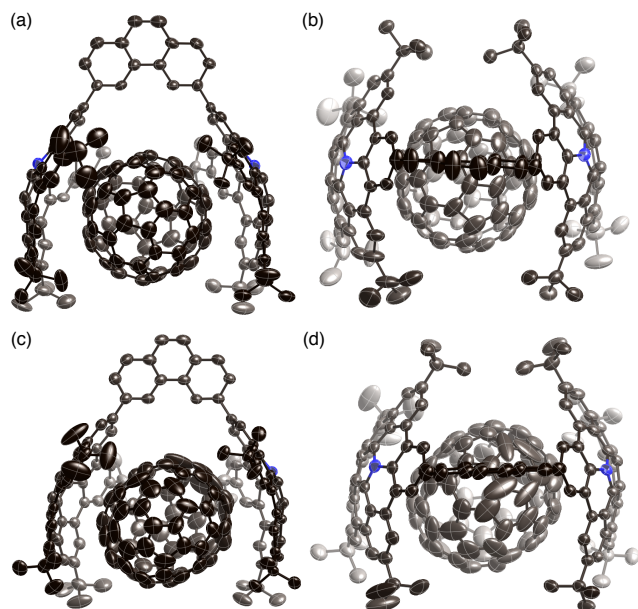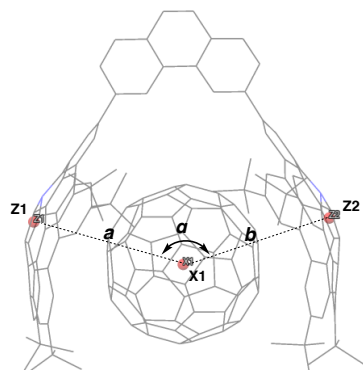
Figure 4. (a) Side and (b) top view of the X-ray crystal structure of **2b•C₆₀** and (c) side and (d) top view of the X-ray crystal structure of **2b•C₇₀**. Thermal ellipsoids are set at 50% probability (hydrogen atoms omitted for clarity).

Table 3. Selected distances and angles of 2b•C₆₀ and 2b•C₇₀.

compounds	distances (Å)		angles (°)
	a	*b*	*α*
2b•C₆₀	6.841	6.815	143.35
2b•C₇₀	7.345	7.055	136.91

To obtain insights into the electronic structure of the hosts and the inclusion complexes, we performed an electrochemical analysis by cyclic voltammetry. Oxidation and reduction potentials for **2a**, **2b**, **2a•C₆₀**, and **2b•C₆₀** were obtained by cyclic voltammetry in CH₂Cl₂ (Figure S16). The obtained potentials are summarized in Table 4. The first oxidation potentials of the complexes were in both cases increased compared to the corresponding hosts. In particular, the first reduction potential of **2b•C₆₀** was observed at –1.28 V, which is shifted to more negative potential than that of pristine C₆₀ (–1.00 V). These results support the existence of significant through-space electronic interactions between **2b** and C₆₀. It is also noteworthy that the first oxidation and reduction potentials of **2b•C₆₀** are reversible, indicating high stability of the com-

plexes during the redox processes. The similar trend was also observed in the case of C₇₀. The first oxidation potentials of host molecules on binding C₇₀ became slightly higher than that for C₆₀.

Table 4. Summarized oxidation and reduction potentials of 2a, 2b, 2b•C₆₀, and 2b•C₆₀.[a]

Compound	E_{ox}^2	E_{ox}^1	E_{red}^1	E_{red}^2
2a	—	0.162	—	—
2b	0.266	0.177	—	—
2a•C₆₀	0.252	0.182	–1.24[c]	—
2b•C₆₀	0.272	0.207	–1.28	–1.44
2a•C₇₀	0.252	0.197	–1.23	–1.48
2b•C₇₀	0.284	0.216	–1.24	–1.51
C₆₀[b]	—	—	–1.00	—
C₇₀[b]	—	—	–0.98	–1.38

a: Potentials are referenced against Fc/Fc⁺; in CH₂Cl₂; *b*: Measured in *o*-dichlorobenzene/acetonitrile; *c*: Determined by differential pulse voltammetry.

Theoretical calculations. The electronic structure of **2b•C₆₀** was further investigated by theoretical calculations. The simulated electronic absorption spectrum of **2b•C₆₀** obtained from time-dependent (TD) DFT calculations at the B3LYP-D3/6-31G(d) level of theory was almost identical to the experimental result. The lowest energy absorption band was attributed to the HOMO–1→LUMO+1 transition (Figure S17). Molecular orbitals (MOs) and energies were obtained from DFT calculations at the same level of theory. Figure 5a illustrates the HOMO–1, and LUMO+1 of **2b•C₆₀**. The HOMO–1 is localized on one of the azabuckybowl units, while the LUMO+1 is located on C₆₀. This result supports the presence of intermolecular charge-transfer interactions. In the case of **2b•C₇₀**, the simulated absorption spectrum indicated that the lowest energy band is attributed as HOMO→LUMO transition (Figure S18). The MOs displayed in Figure 5c and 5d also support the CT characteristic of this transition. The gaseous phase binding geometries of **2a•C₆₀**, **2a•C₇₀**, **2b•C₆₀** and **2b•C₇₀** were optimized by DFT calculations at the same level of theory. In the optimized structures, the orientation of C₇₀ molecule is almost identical to the crystal structure. The sum of calculated Mulliken charge on azabuckybowl units for all complex exhibited positive value, indicating their positively charged characteristics (Table S10). On the other hand, those of fullerenes are negative for **2a•C₇₀**, **2b•C₆₀** and **2b•C₇₀**. These results support that the presence of through-space charge-transfer interaction between two moieties.
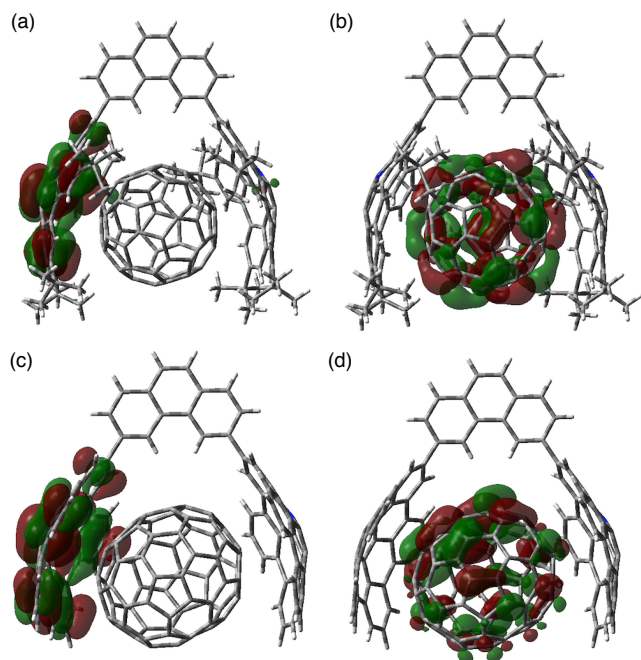
Figure 5. (a) HOMO–1, and (b) LUMO+1 of **2b•C$_{60}$**, and (c) HOMO and (d) LUMO of **2b•C$_{70}$**. These orbitals were calculated at the B3LYP-D3/6-31G(d) level.

Transient absorption and two-photon absorption measurements. To gain further insight into the intermolecular interactions between **2b** and C$_{60}$, we measured the femtosecond transient-absorption (TA) spectra of **2b** and **2b•C$_{60}$** (Figure 6).[25] Upon photoexcitation at 470 nm, obvious changes in the TA spectra of **2b** were not observed relative to its steady-state electronic absorption spectrum. On the other hand, the TA spectra of **2b•C$_{60}$** clearly showed new bands at ca. 530, 690, and 1090 nm, which were assigned to absorption bands of a radical cation of the azabuckybowl unit (530 and 690 nm) and a radical anion of the C$_{60}$ moiety (1090 nm).[16a] This result indicates that the excited-state electron transfer occurs between **2b** and C$_{60}$.[26] In comparison with **2b**, the lifetime of the singlet excited state of **2b•C$_{60}$** (160 ps) decreased upon complexation with C$_{60}$. In particular, the ultrafast rise dynamics (0.6 ps) in the decay profile of **2b•C$_{60}$** indicate electron transfer from the azabuckybowl unit to C$_{60}$. Based on these TA results, we confirmed a photo-induced electron-transfer process in **2b•C$_{60}$**.
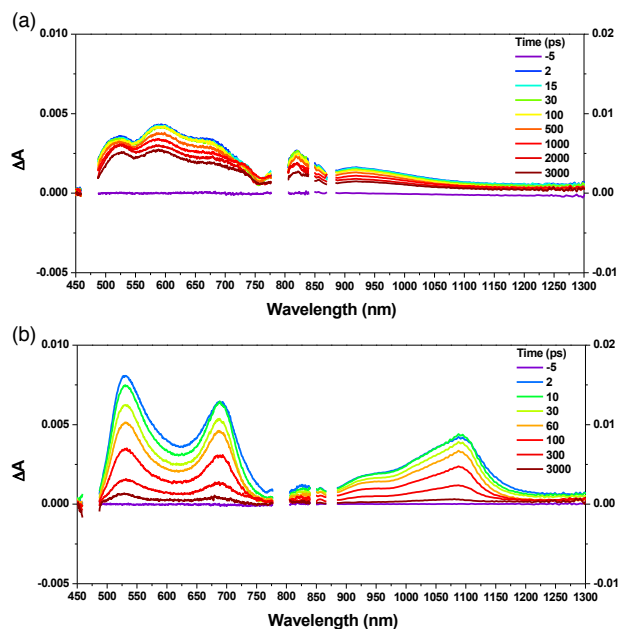

Figure 6. Femtosecond transient-absorption spectra of (a) **2b** and (b) **2b•C$_{60}$** in CH$_2$Cl$_2$ under photoexcitation at 470 nm.

We also measured the TPA cross-section values of **2a**, **2b**, **2a•C$_{60}$**, **2a•C$_{70}$**, **2b•C$_{60}$**, and **2b•C$_{70}$** using a nondegenerate TPA method (Figure 7).[27] We used white light continuum probe pulses as the λ$_2$ pulse to enable the multichannel detection of TPA spectra. The femtosecond near-infrared pump pulse (1600 nm) was used as the λ$_1$ pulse to induce nondegenerate TPA at λ$_1$ + λ$_2$. Negligible TPA cross-section values were observed for the host molecules **2a** and **2b**. Both host exhibited enhancement of TPA cross-sections on binding fullerenes. In particular, apparent enhancement of TPA cross-section were observed for **2b•C$_{60}$** (~200 GM) around 450 nm. The steady-state absorption strength is almost unchanged upon binding, excluding the effect of the first order absorption coefficient upon this TPA enhancement. The TD-DFT calculations indicated that the one-photon absorption band at ~450 nm is attributed to the charge-transfer transition. Accordingly, this result suggests that the formation of a D–A–D electronic supramolecular structure upon binding with C$_{60}$ enhances the third-order nonlinear optical effect. Complex **2b•C$_{70}$** also exhibited enhanced TPA cross-section around 500 nm (200 GM). Although **2a•C$_{60}$** and **2a•C$_{70}$** also showed TPA around 400 nm (~200 GM), the degree of the enhancement was smaller than those with **2b** (~280 GM). This result indicates that **2b** is a more suitable host for generation of TPA characteristic.
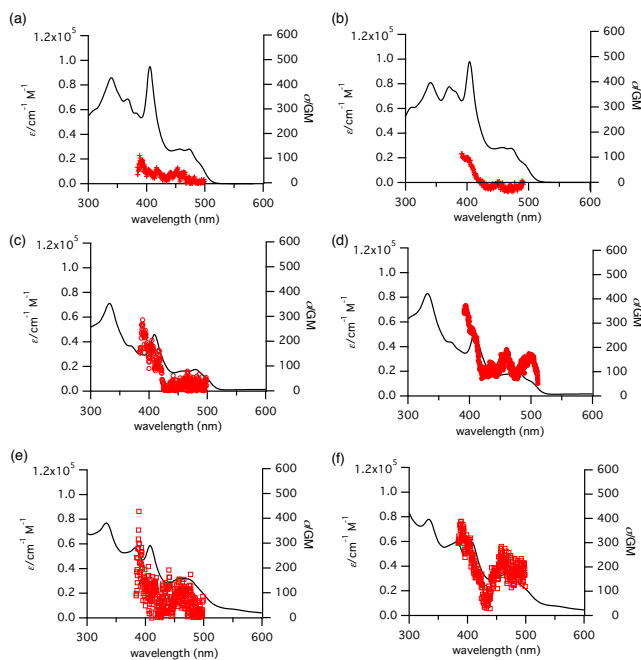
Figure 7. Nondegenerate two-photon absorption spectra of (a) **2a**, (b) **2b**, (c) **2a•C₆₀**, (d) **2b•C₆₀**, (e) **2a•C₇₀**, and (f) **2b•C₇₀** (red marks) along with the corresponding one-photon absorption spectra (black solid lines) in CH₂Cl₂.

Conclusion

In summary, we have designed and prepared two molecular tweezers, which contained two azabuckybowl units that acted as strong fullerene receptors. In the presence of C₆₀ in toluene, both tweezers afforded 1:1 complexes with large intermolecular charge-transfer interactions. The phenanthrene-linked molecular tweezers **2b** exhibited a higher stability in CH₂Cl₂, and could thus be purified by column chromatography on silica gel. These molecular tweezers also captured C₇₀ effectively in solution. The structures of the complexes were clearly determined by X-ray diffraction analysis. Further study by electrochemical and theoretical investigations revealed the presence of through-space charge-transfer interaction between azabuckybowl units and fullerenes, resulting in construction of quadrupolar electronic state. The stability of the complexes enabled us to conduct a non-linear optical analysis, which demonstrated that the supramolecular D–A–D assemblies could have enhanced their TPA properties. These findings in the present research would lead to new design concepts of responsive TPA materials.

ASSOCIATED CONTENT

Supporting Information

Experimental procedures and spectroscopic data, X-ray data, and the results of theoretical calculations. This material is available free of charge via the Internet at http://pubs.acs.org.

AUTHOR INFORMATION

Corresponding Author

hiroto@chembio.nagoya-u.ac.jp; dongho@yonsei.ac.kr; hshino@chembio.nagoya-u.ac.jp

ACKNOWLEDGMENT

REFERENCES

(1) Hardouin-Lerouge, M.; Hudhomme, P.; Sallé, M. *Chem. Soc. Rev.* **2011**, *40*, 30–43.

(2) (a) Leblond, J.; Petitjean, A. *ChemPhysChem*, **2011**, *12*, 1043–1051. (b) Harmata, M. *Acc. Chem. Res.* **2004**, *37*, 862–873. (c) Klärner, F.-G.; Kahlert, B. *Acc. Chem. Res.* **2003**, *36*, 919–932. (d) Petitjean, A.; Khoury, R. G.; Kyritsakas, N.; Lehn, J.-M. *J. Am. Chem. Soc.* **2004**, *126*, 6637–6647. (e) Chen, C. W.; Whitlock, H. W. J. *J. Am. Chem. Soc.* **1978**, *100*, 4921–4922.

(3) (a) Schrader, T.; Bitan, G.; Kläner, F.-G. *Chem. Commun.* **2016**, *52*, 11318–11334. (b) Leblond, J.; Gao, H.; Petitjean, A.; Leroux, J.-C. *J. Am. Chem. Soc.* **2010**, *132*, 8544–8545. (c) Burattini, S.; Greenland, B. W.; Hayes, W.; Mackay, M. E.; Rowan, S. J; Colquhoun, H. M. *Chem. Mater.* **2011**, *23*, 6–8. (d) Tian, Y.-K.; Shi, Y.-G.; Yang, Z.-S.; Wang, F. *Angew. Chem. Int. Ed.* **2014**, *53*, 6090–6094.

(4) (a) Canevet, D.; Pérez, E. M.; Martín, N. *Angew. Chem. Int. Ed.* **2011**, *50*, 9248–9259. (b) Perez, E. M.; Martín, N. *Chem. Soc. Rev.* **2008**, *37*, 1512–1519. (c) Pérez, E. M.; Martín, N. *Pure Appl. Chem.* **2010**, *82*, 523–533.

(5) (a) Atwood, J. L.; Koutsantonis, G. A.; Raston, C. L. *Nature* **1994**, *368*, 229–231. (b) Yoshida, Z.; Takekuma, H.; Takekuma, S.; Matsubara, Y. *Angew. Chem. Int. Ed.* **1994**, *33*, 1597–1599. (c) Moreira, L.; Calbo, J.; Calderon, R. M. K.; Santos, J.; Illescas, B. M.; Arago, J.; Nierengarten, J.-F.; Guldi, D. M.; Orti, E.; Martín, N. *Chem. Sci.* **2015**, *6*, 4426–4432. (d) Constabel, F.; Geckeler, K. E. *Tetrahedron Lett.* **2004**, *45*, 2071–2073. (e) Ogoshi, T.; Ueshima, N.; Sakakibara, F.; Yamagichi, T.; Haino, T. *Org. Lett.* **2014**, *16*, 2896–2899. (f) Pham, D.; Bertran, J. C.; Olmstead, M. M.; Mascal, M.; Balch, A. L. *Org. Lett.* **2005**, *7*, 2805–2808. (g) Fukuzumi, S.; Ohkubo, K.; Kawashima, Y.; Kim, D. S.; Park, J. S.; Jana, A.; Lynch, V. M.; Kim, D.; Sessler, J. L. *J. Am. Chem. Soc.* **2011**, *133*, 15938–15941. (h) Nakamura, T.; Ube, H.; Miyake, R.; Shionoya, M. *J. Am. Chem. Soc.* **2013**, *135*, 18790–18793. (i) Isobe, H.; Hitosugi, S.; Yamasaki, T.; Iizuka, R. *Chem. Sci.* **2013**, *4*, 1293-1297. (j) Haino, T.; Fukunaga, C.; Fukazawa, Y. *Org. Lett.* **2006**, *8*, 3545-3548. (k) Haino, T.; Araki, H.; Fujiwara, Y.; Tanimoto, Y.; Fukazawa, Y. *Chem. Commun.* **2002**, 2148-2149. (l) Haino, T.; Yanase, M.; Fukazawa, Y. *Angew. Chem. Int. Ed. Engl.* **1997**, *36*, 259-260. (m) Haino, T.; Yanase, M.; Fukazawa, Y. *Angew. Chem. Int. Ed.* **1998**, *37*, 997-998. (n) Shoji, Y.; Tashiro, K.; Aida, T. *J. Am. Chem. Soc.* **2004**, *126*, 6570–6571. (o) Mulla, K.; Shalik, H.; Thompson, D. W.; Zhao, Y. *Org. Lett.* **2013**, *15*, 4532–4535. (p) Cao, J.; Zhu, X.-Z.; Chen, C.-F. *J. Org. Chem.* **2010**, *75*, 7420–7423.

(6) (a) Tashiro, K.; Aida, T. *Chem. Soc. Rev.* **2007**, *36*, 189–197. (b) Boyd, P. D. W.; Reed, C. A. *Acc. Chem. Res.* **2005**, *38*, 235–242. (c) Durot, S.; Taesch, J.; Heitz, V. *Chem. Rev.* **2014**, *114*, 8542–8578. (d) Garcia-Simon, C.; Costas, M.; Ribas, X. *Chem. Soc. Rev.* **2016**, *45*, 40–62. (e) Uno, H.; Furukawa, M.; Fujimoto, A.; Uoyama, H.; Watanabe, H.; Okujima, T.; Yamada, H.; Mori, S.; Kuramoto, M.; Iwamura, T.; Hatae, N.; Tani, F.; Komatsu, N. *J. Porphyrins Phthalocyanines* **2011**, *15*, 951–963.

(7) For recent examples of porphyrin-based fullerene hosts, see: (a) Ke, X.-S.; Kim, T.; Brewster, II, J. Y.; Lynch, V. M.; Kim, D.; Sessler, J. L. *J. Am. Chem. Soc.* **2017**, *139*, 4627–4630. (b) Moreira, L.; Calbo, J.; Aragó, J.; Illescas, B. M.; Nierengarten, I.; Delavaux-Nicot, B.; Ortí, E.; Martín, N.; Nierengarten, J.-F. *J. Am. Chem. Soc.* **2016**, *138*, 15359–15367. (c) Saegusa, Y.; Ishizuka, T.; Kojima, T.; Mori, S.; Kawano, M.; Kojima, T. *Chem.-Eur. J.* **2015**, *21*, 5302–5306. (d) Ortiz, M.; Cho, S.; Niklas, J.; Kim, S.; Poluektov, O. G.; Zhang, W.; Rumbles, G.; Park, J. *J. Am. Chem. Soc.* **2017**, *139*, 4286–4289. (e) Song, J.; Aratani, N.; Shinokubo, H.; Osuka, A. *J. Am. Chem. Soc.* **2010**, *132*, 16356–16357. (f) Meng, W.; Breiner, B.; Rissanen, K.; Thoburn, J. D.; Clegg, J. K.; Nitschke, J. R. *Angew. Chem. Int. Ed.* **2011**, *50*, 3479–3483.

(8) Rossom, W. V.; Kundrát, O.; Ngo, T. H.; Lhoták, P.; Dehaen, W.; Maes, W. *Tetrahedron Lett.* **2010**, *51*, 2423–2426.

(9) (a) Sańchez-Molina, I.; Grimm, B.; KrickCalderon, R. M.; Claessens, C. G.; Guldi, D. M.; Torres, T. *J. Am. Chem. Soc.* **2013**, *135*, 10503–10511. (b) Sanchez-Molina, I.; Claessens, C. G.; Grimm, B.; Guldi, D. M.; Torres, T. *Chem. Sci.* **2013**, *4*, 1338–1344. (c) Shimizu, S.; Nakano, S.; Hosoya, T.; Kobayashi, N. *Chem. Commun.* **2011**, *47*, 316–318. (d) Nakano, S.; Kage, Y.; Furuta, H.; Kobayashi, N.; Shimizu, S. *Chem.-Eur. J.* **2016**, *22*, 7706–7710.

(10) (a) Yoshida, K.; Osuka, A. *Chem. Asian J.* **2015**, *10*, 1526–1534. (b) Yoshida, K.; Osuka, A. *Chem.-Eur. J.* **2016**, *22*, 9396–9403.

(11) (a) Yamada, M.; Ohkubo, K.; Shionoya, M.; Fukuzumi, F. *J. Am. Chem. Soc.* **2014**, *136*, 13240–13248. (b) Mizyed, S.; Georghiou, P. E.; Bancu, M.; Cuadra, B.; Rai, A. K.; Cheng, P.; Scott, L. T. *J. Am. Chem. Soc.* **2001**, *123*, 12770–12774. (c) Georghiou, P. E.; Tran, A. H.; Mizyed, S.; Bancu, M.; Scott, L. T. *J. Org. Chem.* **2005**, *70*, 6158–6163. (d) Liu, Y.-M.; Xia, D.; Li, B.-W.; Zhang, Q.-Y.; Sakurai, T.; Tan, Y,-Z.; Seki, S.; Xie, S.-Y.; Zheng, L.-S. *Angew. Chem. Int. Ed.* **2016**, *55*, 13047–13051.

(12) (a) Huerta, E.; Isla, H.; Pérez, E. M.; Bo, C.; Martín, N.; Mendoza, J. *J. Am. Chem. Soc.* **2010**, *132*, 5351–5353. (b) Ghiassi, K. B.; Chen, S. Y.; Prinz, P.; Meijere, A.; Olmstead, M. M.; Balch, A. L. *Cryst. Growth Des.* **2014**, *14*, 4005–4010. (c) Georghiou, P. E.; Dawe, L. N.; Tran, H.-A.; Strübe, J.; Neumann, B.; Stammier, H.-G.; Kuck, D. *J. Org. Chem.* **2008**, *73*, 9040–9047. (d) Filatov, A. S.; Ferguson, M. V.; Spisak, S. N.; Li, B.; Campana, C. F.; Petrukhina, M. A. *Cryst. Growth Des.* **2014**, *14*, 756–762. (e) Isla, H.; Gallego, M.; Pérez, E. M.; Viruela, R.; Ortí, E.; Martín, N. *J. Am. Chem. Soc.* **2010**, *132*, 1772–1773.

(13) (a) Sygula, A.; Collier, W. E. In *Fragments of Fullerenes and Carbon Nanotubes: Designed Synthesis, Unusual Reactions, and Coordination Chemistry*, Petrukhina, M. A.; Scott, L. T. Eds. Wiley-VCH, Weinheim, **2011**, Chapter 1. (b) Sygula, A. *Synlett* **2016**, *27*, 2070.

(14) (a) Sygula, A.; Fronczek, F. R.; Sygula, R.; Rabideau, P. W.; Olmstead, M. M. *J. Am. Chem. Soc.* **2007**, *129*, 3842–3843. (b) Le, V. H.; Yanney, M.; McGuire, M.; Sygula, A.; Lewis, E. A. *J. Phys. Chem. B* **2014**, *118*, 11956–11964. (c) Yanney, M.; Fronczek, F. R.; Sygula, A. *Angew. Chem. Int. Ed.* **2015**, *54*, 11153–11156. (d) Kuragama, P. L. A.; Fronczek, F. R.; Sygula, A. *Org. Lett.* **2015**, *17*, 5292–5295. (e) Kumarasinghe, K. G. U. R.; Fronczek, F. R.; Valle, H. U.; Sygula, A. *Org. Lett.* **2016**, *18*, 3054–3057. (f) Yanney, M.; Sygula, A. *Tetrahedron Lett.* **2013**, *54*, 2604–2607.

(15) (a) Álvarez, C. M.; Aullón, G.; Barbero, H.; García-Escudero, L. A.; Martínez-Pérez, C.; Martín-Álvarez, J. M.; Miguel D. *Org. Lett.* **2015**, *17*, 2578–2581. (b) Yang, D.-C.; Li, Meng, Chen, C.-F. *Chem. Commun.* **2017**, *53*, 9336–9339.

(16) (a) Yokoi, H.; Hiraoka, Y.; Hiroto, S.; Sakamaki, D.; Seki, S.; Shinokubo, H. *Nat. Commun.* **2015**, *6*, 8215. (b) Ito, S.; Tokimaru, Y.; Nozaki, K. *Angew. Chem. Int. Ed.* **2015**, *54*, 7256–7260.

(17) Albota, M.; Beljonne, D.; Brédas, J.-L.; Ehrlich, J. E.; Fu, J.-Y.; Heikal, A. A.; Hess, S. E.; Kogej, T.; Levin, M. D.; Marder, S. R.; MacCord-Maughon, D.; Perry, J. W.; Röckel, H.; Rumi, M.; Subramaniam, G.; Webb, W. W.; Wu, X.-L.; Xu, C. *Science* **1998**, *281*, 1653–1656.

(18) (a) Ogawa, K.; Ohashi, A.; Kobuke, Y.; Kamada, K.; Ohta, K. *J. Phys. Chem. B* **2005**, *109*, 22003–22012. (b) Tanihara, J.; Ogawa, K.; Kobuke, Y. *J. Photochem. Photobiol. A* **2006**, *178*, 140–149.

(19) (a) Chakrabarti, S.; Ruud, K. *J. Phys. Chem. A* **2009**, *113*, 5485–5488. (b) Chakrabarti, S.; Ruud, K. *Phys. Chem. Chem. Phys.* **2009**, *11*, 2592–2596. (c) Beerepoot, M. T. P.; Friese, D. J.; Ruud, K. *Phys. Chem. Chem. Phys.* **2014**, *16*, 5958–5964.

(20) (a) Sun, D.; Tham, F. S.; Reed, C. A.; Chaker, L.; Burgess, M.; Boyd, P. D. W. *J. Am. Chem. Soc.* **2000**, *122*, 10704–10705. (b) Sun, D.; Tham, F. S.; Reed, C. A.; Chaker, L.; Boyd, P. D. W. *J. Am. Chem. Soc.* **2002**, *124*, 6604–6612.

(21) (a) Yanagisawa, M.; Tashiro, K.; Yamasaki, M.; Aida, T. *J. Am. Chem. Soc.* **2007**, *129*, 11912–11913. (b) Tashiro, K.; Aida, T.; Zheng, J.-Y.; Kinbara, K.; Saigo, K.; Sakamoto, S.; Yamaguchi, K. *J. Am. Chem. Soc.* **1999**, *121*, 9477–9478. (c) Ouchi, A.; Tashiro, K.; Yamaguchi, K.; Tsuchiya, T.; Akasaka, T.; Aida, T. *Angew. Chem. Int. Ed.* **2006**, *45*, 3542–3546.

(22) (a) Álvarez, C. M.; García-Escudero, L. A.; García-Rodriguez, R.; Martín-Álvarez, J. M.; Miguel, D.; Rayón, V. M. *Dalton Trans.* **2014**, *43*, 15693–15696. (b) Mück-Lichtenfeld, C.; Grimme, S.; Kobryn, L.; Sygula, A. *Phys. Chem. Chem. Phys.* **2010**, *12*, 7091–7097.

(23) (a) Kawase, T. In *Supramolecular Chemistry of Fullerenes and Carbon Nanotube*, Martin, N.; Nierengarten, J.-F. Eds. Wiley-VCH, Weinheim, **2012**, pp. 55-78. (b) Kawase, T. *Chem. Rev.* **2006**, *106*, 5250–5273.

(24) (a) Yamamura, M.; Saito, T.; Nabeshima, T. *J. Am. Chem. Soc.* **2014**, *136*, 14299–14306. (b) Yamada, M.; Ohkubo, K.; Shionoya, M.; Fukuzumi, S. *J. Am. Chem. Soc.* **2014**, *136*, 13240–13248. (d) Zhou, Z.; Qin, Y.; Zhu, Q. *Chem. Commun.* **2014**, *50*, 4082–4084. (e) Iwamoto, T.; Watanabe, Y.; Sadahito, T.; Haino, T.; Yamago, S. *Angew. Chem. Int. Ed.* **2011**, *50*, 8342–8344.

(25) (a) Calderon, R. M. K.; Valero, J.; Grimm, B.; Mendoza, J.; Guldi, D. M. *J. Am. Chem. Soc.* **2014**, *136*, 11436–11443. (b) Pal, D.; Furukawa, M.; Komatsu, N.; Uno, H.; Bhattacharya, S. *Spectrochimica Acta Part A* **2018**, *78*, 185–190. (c) Mukheriee, S.; Bauri, A. K.; Bhattacharva, S. *Chem. Phys. Lett.* **2010**, *500*, 128–139.

(26) Ke, X.-S.; Kim, T.; Brewster II, J. T.; Lynch, V. M.; Kim, D.; Sessler, J. L. *J. Am. Chem. Soc.* **2017**, *139*, 4627–4630.

(27) (a) Yamaguchi, S.; Tahara, T. *Chem. Phys. Lett.* **2003**, *376*, 237–243. (b) Lee, S.; Kim, D. *J. Phys. Chem. A* **2016**, *120*, 9217–9223.

For C$_{60}$
X = -CH=CH-

Molecular Tweezers

For C$_{70}$
X = -NH-

Two-Photon Absorbing
D-A-D Systems